



# Forecasting Large Hail and Lightning using Additive Logistic Regression Models and the ECMWF Reforecasts

Francesco Battaglioli<sup>1,2</sup>, Pieter Groenemeijer<sup>1,3</sup>, Ivan Tsonevsky<sup>4</sup>, Tomáš Púčik<sup>3</sup>

<sup>1</sup>European Severe Storms Laboratory e.V. (ESSL), Wessling, 82234, Germany

5 <sup>2</sup>Institut für Meteorologie, Freie Universität Berlin, Berlin, 12165, Germany

<sup>3</sup>European Severe Storms Laboratory (ESSL) – Science and Training, Wiener Neustadt, 2700, Austria

<sup>3</sup>European Centre for Medium Range Weather Forecasts (ECMWF), Reading, RG2 9AX, United Kingdom

*Correspondence to:* Francesco Battaglioli (francesco.battaglioli@essl.org)

10 **Abstract.** Additive Logistic Regression models for lightning and large hail ( $AR_{hail}$ ) were developed using convective parameters from the ERA5 reanalysis, hail reports from the European Severe Weather Database (ESWD), and lightning observations from the Met Office Arrival Time Difference network (ATDnet). The model yields the probability of large hail in a given timeframe over a particular grid point and can accurately reproduce the climatological distribution and the seasonal cycle of observed hail events in Europe. To explore the value of this approach to medium-range forecasting, a similar four-  
15 dimensional model was developed using predictor parameters retrieved from ECMWF reforecasts: Most Unstable CAPE, 925 – 500 hPa bulk shear, Mixed Layer Mixing Ratio, and the Wet Bulb Zero Height. This model was applied to the ECMWF reforecasts to compute probabilistic large hail forecasts for all available 11 ensemble members, from 2008 to 2019 and for lead times up to 228 hours. First, we compared the hail ensemble forecasts for different lead times with observed hail occurrence from the ESWD focusing on a recent hail outbreak. Secondly, we evaluated the model's predictive skill as a function of forecast  
20 lead time using the Area under the ROC Curve (AUC) as a validation score. This analysis showed that  $AR_{hail}$  has a very high predictive skill ( $AUC > 0.95$ ) for a lead time up to 60 hours.  $AR_{hail}$  retains a high predictive skill even for extended forecasts ( $AUC = 0.86$  at 180 hours lead time). Finally, the performance of the four-dimensional model was compared with that of composite parameters such as the Significant Hail Parameter (SHP) or the product of CAPE and the 925 – 500 hPa bulk shear (CAPESHEAR). Results show that  $AR_{hail}$  outperformed CAPESHEAR at all lead times and SHP at short to medium lead  
25 times. This suggests that the combination of Additive Logistic Regression models and ECMWF ensemble forecasts can create highly skilful medium-range hail forecasts for Europe.

## 1 Introduction

Single hailstorms have been shown to cause more than 1 billion US dollars in damage across several regions of the world including Europe, the United States and Australia (Chagnon et al. 2009; Púčik et al. 2019; Warren et al. 2020). Such extensive  
30 economic impacts have sparked research on different aspects of hailstorms ranging from the development of hail climatologies



(Cintineo et al. 2012; Cecil and Blankenship 2012; Bang and Cecil 2019; Púčik et al. 2019; Taszarek et al. 2020a; Fluck et al. 2021; Murillo et al. 2021) to forecasting (Jewell and Brimelow 2009; Adams-Selin and Ziegler 2016; Czernecki et al. 2019; Allen et al. 2020) and nowcasting (Nisi et al. 2020; Schmidt 2020; Ryzkhov et al. 2013; Ortega et al. 2016). In the United States, research has also focused on forecasting hail using convective allowing models (CAMs, Gallo et al. 2016, 2018) and  
35 convective allowing ensembles (Loken et al. 2020). In Europe, hail forecasting research has mostly concentrated on (semi-) automatic nowcasting techniques using radar data (Martius et al. 2015). Although successful medium-range hail forecasts can mitigate the impacts of hail and have been shown to be skilful in the United States (Lepore et al. 2017, 2018), little attention has been given to the development of specific products for medium-range hail forecasting in Europe. At such lead times, convection allowing models are not available, but an ingredients-based approach (Doswell et al. 1996) can be used, whereby  
40 forecasters look for the simultaneous presence of prerequisites needed to sustain hailstorms, such as instability, moisture, lift, and a minimum amount of wind shear. Composite parameters such as the Large Hail Parameter (LHP; Johnson and Sugden 2014), the Supercell Composite Parameter (SCP; Thompson et al. 2004) and the Significant Hail Parameter (SHP; [http://www.spc.noaa.gov/exper/mesoanalysis/help/help\\_sigh.html](http://www.spc.noaa.gov/exper/mesoanalysis/help/help_sigh.html)) can help by combining several ingredients into one number describing whether the environmental conditions are supportive for large hail and can be used for medium-range forecasting.  
45 SHP calculated from the Global Ensemble Forecast System (GEFS) yielded skilful probabilistic hail forecasts up to 12 days in advance in the United States (Gensini and Tippet, 2019). Although composite parameters such as SHP perform well across the United States, climatologies based on them perform worse across regions where the parameter has not been specifically developed (e.g., Europe as found by Taszarek et al. 2020b). Battaglioli et al. (2023) showed that the Additive Logistic Regression Models (AR-CHaMo) for large hail occurrence have a better predictive skill than SHP and can result in a more  
50 realistic climatological distribution of hail occurrence across Europe. Building upon these findings, in this study we leverage an ensemble approach in conjunction with the lightning and hail models from Battaglioli et al. (2023) to yield probabilistic lightning and hail forecasts with the ultimate goal of improving medium-range forecasting of these hazards across Europe.

## 2 Data

### 2.1 AR-CHaMo lightning and hail models

55 The AR-CHaMo models were developed by Rädler et al. (2019) and improved by Battaglioli et al. (2023). The models were trained using lightning observations from the Arrival Time Difference Network (ATDNet, Anderson and Klugmann 2014; Enno et al. 2020), hail reports from the European Severe Weather Database (ESWD; Dotzek et al. 2009; Groenemeijer et al. 2017) and convective parameters from the ERA5 reanalysis (Hersbach et al. 2020). They use logistic regression to assign a probability of hazard occurrence as a function of reanalysis-derived predictor parameters. AR-CHaMo separately predicts the  
60 probability of thunderstorm formation and the probability of large hail ( $\geq 2$  cm) given that a thunderstorm formed. The probability of large hail ( $P_{\text{hail}>2\text{cm}}$ ) is a product of these two components as shown in Eq. (1):

$$P_{\text{hail}>2\text{cm}} = P_{\text{lightning}} \cdot P_{\text{hail}>2\text{cm}|\text{lightning}} \quad (1)$$



Different predictor parameters from the ERA5 reanalysis were selected for the lightning model and for the hail model following  
65 a model selection procedure based on an ingredients-based approach. More details on the model selection can be found in  
Battaglioli et al. (2023) while the final model predictors are listed in Table 1.

## 2.2 ECMWF forecast data

Forecast data across Europe were obtained from ECMWF reforecasts (Vitart, 2014) for the period 2008-2019. ECMWF  
reforecasts used in this study consist of 10 perturbed ensemble members and 1 control forecast run every Monday and  
70 Thursday. These reforecasts, unlike reanalysis, always use the operational version of ECMWF's Integrated Forecasting System  
(IFS), covering two IFS cycles: 46r1 till 30 June 2020 and 47r1 afterwards. Reforecast data were extracted at a spatial  
resolution of  $0.2^\circ \times 0.2^\circ$  and 6-hourly temporal resolution. The forecast parameters downloaded from reforecasts were  
temperature, specific humidity, u and v wind components at the 1000, 850, 700 and 500 hPa pressure levels. They were used  
to compute convection related parameters such as mixing ratio, mid-level relative humidity, 925 to 500 hPa bulk shear (deep  
75 layer shear). Composite parameters, such as CAPE-shear (a product of  $\sqrt{CAPE}$  and deep layer shear) and SHP were also  
calculated while CAPE for the most-unstable parcel (MUCAPE) and convective precipitation were obtained directly from the  
IFS.

## 2.3 Lightning observations and hail reports

Lightning data from ATDnet were used to verify lightning forecasts from AR-CHaMo. This network can detect lightning  
80 flashes even at large distances from a sensor and allows verification of the lightning forecasts across a broad region covering  
most of Europe. Data was obtained for the period 2008–2019, gridded on a  $0.2^\circ \times 0.2^\circ$  box to allow for direct comparison to  
ECMWF reforecasts, and organized as a binary field indicating whether a lightning case occurred (1 = yes, 0 = no). A lightning  
case was defined as a one-hour period with at least 2 lightning strikes per grid box. Following Rädler et al. (2019), single  
detections were ignored as they might be isolated measurement errors rather than lightning. Hail reports were obtained from  
85 the ESWD and used to verify the hail forecasts. As per Rädler et al. (2019), reports with an excessive time uncertainty ( $> 1$   
hour) were discarded from the verification dataset.

## 3 Model development and adaptation

The models for lightning and large hail developed in Battaglioli et al. 2023 were based on the predictors from the ERA5  
reanalysis listed in Table 1. Owing to the limited vertical resolution of the ECMWF reforecast data, some of the original AR-  
90 CHaMo predictors (e.g., MU500\_CAPE-10°) could not be calculated using the ECMWF reforecasts. For this reason, the  
models were adapted using predictors as close as possible to their original versions (e.g., MU\_CAPE was chosen instead of  
MU500\_CAPE-10°). The models were then trained again using the adapted predictors (shown in Table 2) using ERA5



reanalysis, lightning and hail observations. The models assign a probability of hazard occurrence as a function of the reanalysis-derived predictor parameters listed in Table 2 to any location in a  $0.25^\circ \times 0.25^\circ$  grid and 1 hourly intervals. Given the different spatial (ERA5:  $0.25^\circ \times 0.25^\circ$ , ECMWF reforecast:  $0.20^\circ \times 0.20^\circ$ ) and temporal (1 hour, 6 hours) resolution between ERA5 and ECMWF reforecasts, the probabilities had to be recalibrated. To account for the different spatial resolution of ECMWF reforecasts, the ERA5  $P_{hazard(ERA5)}$  probabilities were adapted following Eq. (2):

$$P_{hazard(ECMWF)} = 1 - (1 - P_{hazard(ERA5)})^{A_{ECMWF}/A_{ERA5}} \quad (2)$$

100

Where:

$A_{ECMWF}$  is the Area of an ECMWF reforecast grid box ( $km^2$ )

$A_{ERA5}$  is the Area of an ERA5 grid box ( $km^2$ )

$P_{hazard(ECMWF)}$  is the calibrated probability using an ECMWF reforecast grid (%)

105

Given that ECMWF reforecasts are available every 6 hours, large hail probabilities could be calculated only at 4 different hourly time steps during the day (00-01, 06-07, 12-13, 18-19 UTC). Using only 4 hourly time steps would significantly limit the amount of large hail reports to work with. Therefore, probabilities were upscaled to three-hour intervals (00-03, 06-09, 12-15, 18-21 UTC) following Eq. (3):

110

$$P_{hazard(3\text{ hourly})} = 1 - (1 - P_{hazard(1\text{ hourly})})^3 \quad (3)$$

With these adaptations, we applied the AR-CHaMo based on ERA5 to ECMWF reforecasts yielding ensemble lightning and hail forecasts for the period 2008-2019 for the whole of Europe.

## 115 4 Application of hail and lightning model to a case study: 15<sup>th</sup> of June 2019

### 4.1 Ensemble Forecasts

We first tested the AR-CHaMo-based lightning and hail forecasts on a case study. On the 15<sup>th</sup> of June 2019, severe storms with large hail occurred in eastern Germany, western-Poland and western Czechia. More than 20 hail reports were submitted for the period of 12–15 UTC with several hail reports exceeding 5 cm in diameter. A second region of interest on the day was south-eastern France where very large hail was also reported (8 cm near Grenoble). We evaluated the performance of the ensemble forecasts depending on the lead time by considering ECMWF reforecasts initialized at three different lead times (T-12h, T-108h and T-180h) ahead of the event. To allow for a comparison with hail forecast products from the U.S. Storm Prediction Centre (SPC), probabilities were upscaled to yield a probability of hail  $\geq 2$  cm occurrence in a radius of 25 miles of a point, approximately 40 km. For hail forecasts for the 15<sup>th</sup> of June 2019 at 12 UTC, initialized at 00 UTC on the same day,

120



125 a strong agreement between all ensemble members was present in identifying the German-Poland-Czechia region and south-  
eastern France as the areas with highest hail potential ( $P_{\text{hail}>2\text{cm}} > 30\%$ ) (Figure 1).

Similarly to the hail forecasts, there was a strong agreement in lightning forecasts among the ensemble members at 12 hours  
lead time (Figure 2). A high probability of lightning ( $P_{\text{lightning}} > 80\%$ ) was present across the German-Polish border and across  
south-eastern France This means that the conditional probability of hail given the presence of thunderstorms ( $P_{\text{hail}>2\text{cm}|\text{lightning}}$ )  
130 must have been higher here than over Germany as the hail probabilities were similar over both regions. Between 12 and 15  
UTC, widespread lightning activity occurred across a broad region extending from Northern Germany and Denmark all the  
way south to southern Austria, verifying the lightning forecast in these areas. In addition to these regions, high lightning  
probabilities were found along a corridor extending from Ukraine into Russia. Widespread lightning activity was also observed  
here. An underestimation of the lightning activity was present across western Türkiye, where thunderstorms occurred despite  
135 low CAPE ( $< 100\text{ J/kg}$ ; see sounding in Appendix A).

#### 4.2 Physical interpretation of model forecasts

Forecast soundings and hodographs can show how individual parameters influenced the probability of lightning or hail  
simulated by AR-CHaMo. Two regions, central Ukraine and central Italy, showed respectively high and low probabilities  
lightning (Figure 3). While moderate buoyancy ( $\text{CAPE} > 1000\text{ Jkg}^{-1}$ ) was present in both regions, the main difference in the  
140 two profiles was the mid-level relative humidity, significantly lower in the Italian sounding. Here a deep, dry layer in the mid-  
troposphere could have resulted in dry air entrainment of updrafts that inhibited convective initiation (Rädler et al. 2019,  
Poręba et al. 2022). The comparison between hail and lightning forecasts highlights the model's ability to distinguish between  
regions with lightning potential and with hail potential. In a region extending from Romania into Ukraine and Russia, low  
probabilities of large hail ( $P_{\text{hail}>2\text{cm}} < 10\%$ ) were found (Figure 4) alongside high lightning probabilities ( $P_{\text{lightning}} > 70\%$ ). On  
145 the other hand, across eastern Germany the probabilities of lightning ( $P_{\text{lightning}} > 70\%$ ) and hail ( $P_{\text{hail}>2\text{cm}} > 25\%$ ) were both  
high. While high CAPE was present both across Ukraine and eastern Germany, the deep-layer shear was much stronger over  
Germany. Stronger shear is associated with a higher likelihood of large hail, because it promotes storm organisation (Thompson  
et al. 2012; Johnson and Sugden 2014; Púčik et al. 2015; Taszarek et al. 2020b; Kumjian et al. 2021). This was well reflected  
by AR-CHaMo that showed a higher hail probability across eastern Germany in correspondence with the strongest shear.

#### 150 4.3 Forecast dependence on lead time

We next investigated how lead time affects forecast performance by comparing the forecast for the 15<sup>th</sup> of June 2019 at 12  
UTC initialised on the 11<sup>th</sup> of June 2019 at 00 UTC (T-108 h, Figure 5) with the T-12h forecast (Figure 1). Despite the increased  
lead time, the ensemble members were still in good agreement regarding the location of the highest hail probabilities across  
the German-Polish-Czech area even 4 days in advance. The largest difference compared to the T-12-hour forecast was found  
155 across south-eastern France where most members showed no probability of large hail occurrence.



The reason for the large spread in the hail probabilities was a large spread in the predicted CAPE (Figure 7), which was much lower for shorter lead times (Figure 6). While the T-12-hour forecast highlights a localised spot of high CAPE across south-eastern France, this region of enhanced buoyancy was not represented by most members in the T-108-hour forecast. Forecasts of deep-layer shear (not shown) for the two lead times did not show differences that might impact the forecast across south-eastern France. As the lead time and spread among the forecast members increased, the probabilities decreased (Figure 8).  
160 Despite the increased spread compared to the T-12-hour forecast, the T-108-hour hail forecast had a good predictive skill across the German-Polish-Czech area with a widespread 10 – 15 % probability of occurrence, that could be clearly distinguished from surrounding areas with very low probabilities. The T-108-hour lightning forecast (Appendix B) was also in good agreement with the T-12-hour forecast, although lower confidence was found across Eastern Europe where uncertainty  
165 regarding the location of the initiation boundary existed. The spread increased further in the T-180-hour forecast for both hail and lightning (Figure 8). From this case study we showed that the logistic model applied to the ECMWF reforecasts provided a skilful forecast at least up to 108 hours in advance for both hail and lightning. The loss of predictive skill from 12 to 108 hours for the hail model was mostly caused by an increasing uncertainty in the CAPE forecast with increasing lead time.

## 5 Model Application

The ensemble mean probabilistic forecasts were systematically verified at four different times during the day (00UTC, 06  
170 UTC, 12UTC, 18UTC) against lightning observations from ATDnet in the one hour following the forecast time (00–01 UTC, 06–07 UTC, 12–13 UTC, 18–19 UTC) and hail reports from the ESWD in the three hours following the forecast time (00–03UTC, 06–09UTC, 12–15UTC, 18–21UTC). While for lightning the full European domain (Figure 1) was used to verify lightning forecasts owing to the homogenous detection efficiency of ATDnet across the domain, hail forecasts were only  
175 verified against ESWD hail reports in Central Europe. This reduced area was chosen because of a lack of reports from some regions, such as south-eastern Europe (Rädler et al. 2019). We used the Receiver Operating Characteristic (ROC) curves for lead times from 12 to 228 hours (at 24-hour time steps) to investigate changes in forecast skill of the lightning and hail models, similarly to Tsonevsky et al. (2018). The Area Under the ROC Curve (AUC) scores for the hail model were higher than the lightning model ones at all lead times (Figure 9). The hail model exhibited a very high predictive skill:  $AUC > 0.95$  for lead  
180 times up to 60 hours. Although the predictive skill decreased with increasing lead time, a high AUC was still found for lead times up to 108 hours. A relatively strong discontinuity in predictive skill was found between 108 (0.920) and 132 hours (0.873) and after 180 hours. The lightning model exhibited an almost linear decrease of predictive skill with increasing lead time. The performance of  $AR_{hail}$  was compared with that of 1-dimensional logistic models trained using CAPE-shear and SHP as predictors. In Figure 10, we displayed the AUC scores for  $AR_{hail}$  and for the models based on the two composite parameters  
185 as a function of the forecast lead time. To quantify the uncertainty in the AUC for the different models we performed a 1000-member block bootstrap procedure as done by Hamill et al. (2018) that allowed us to determine the corresponding 95% confidence intervals (Figure 10). Comparing the AUC scores of the probabilistic forecasts based on the 1-dimensional CAPESHEAR model and those of  $AR_{hail}$ , we concluded that  $AR_{hail}$  outperformed CAPESHEAR at all lead times. Compared

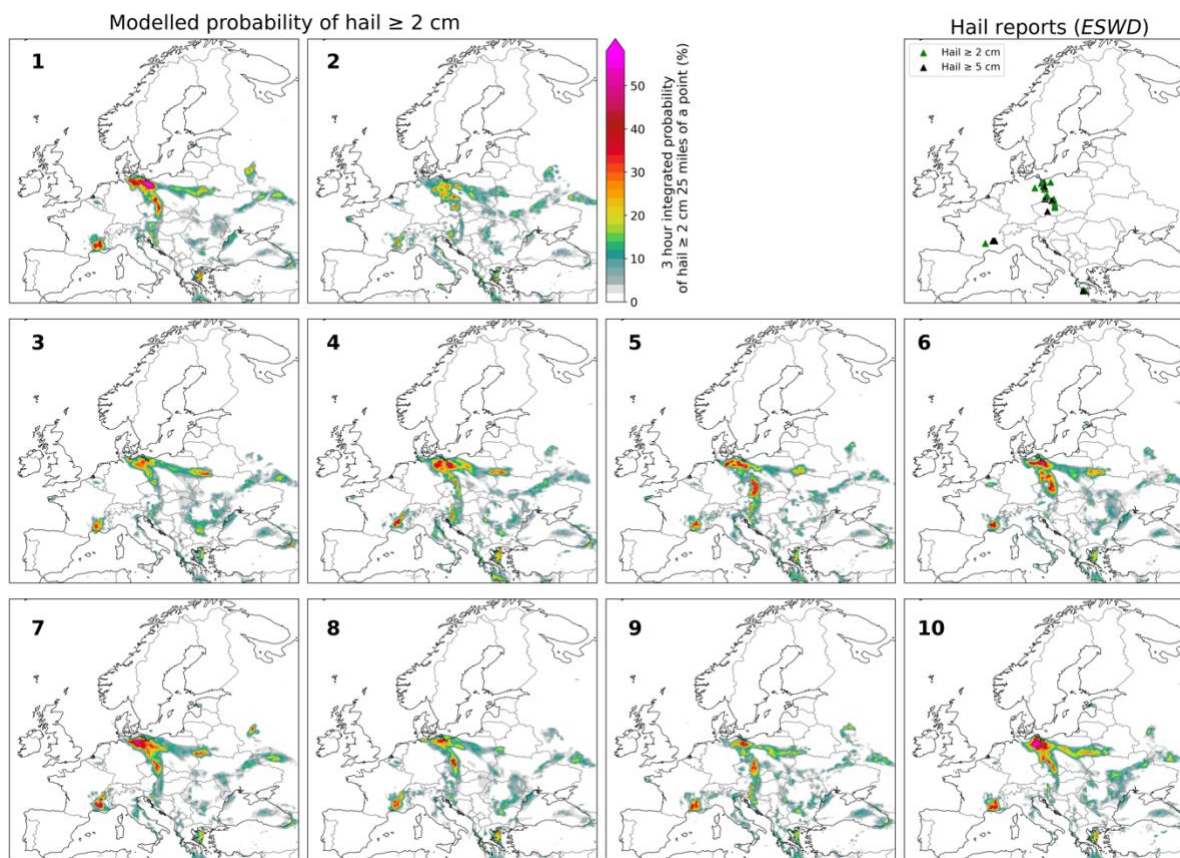


190 to SHP,  $AR_{hail}$  had a higher performance at short-to-medium range (up to 60-84 hours) while with increasing lead time the two metrics became comparable in terms of predictive skill. It is hypothesised that the increase in the uncertainty of the atmospheric predictors was responsible for the loss of skill with increasing lead time, as shown for CAPE in Section 1.

## 6 Conclusion

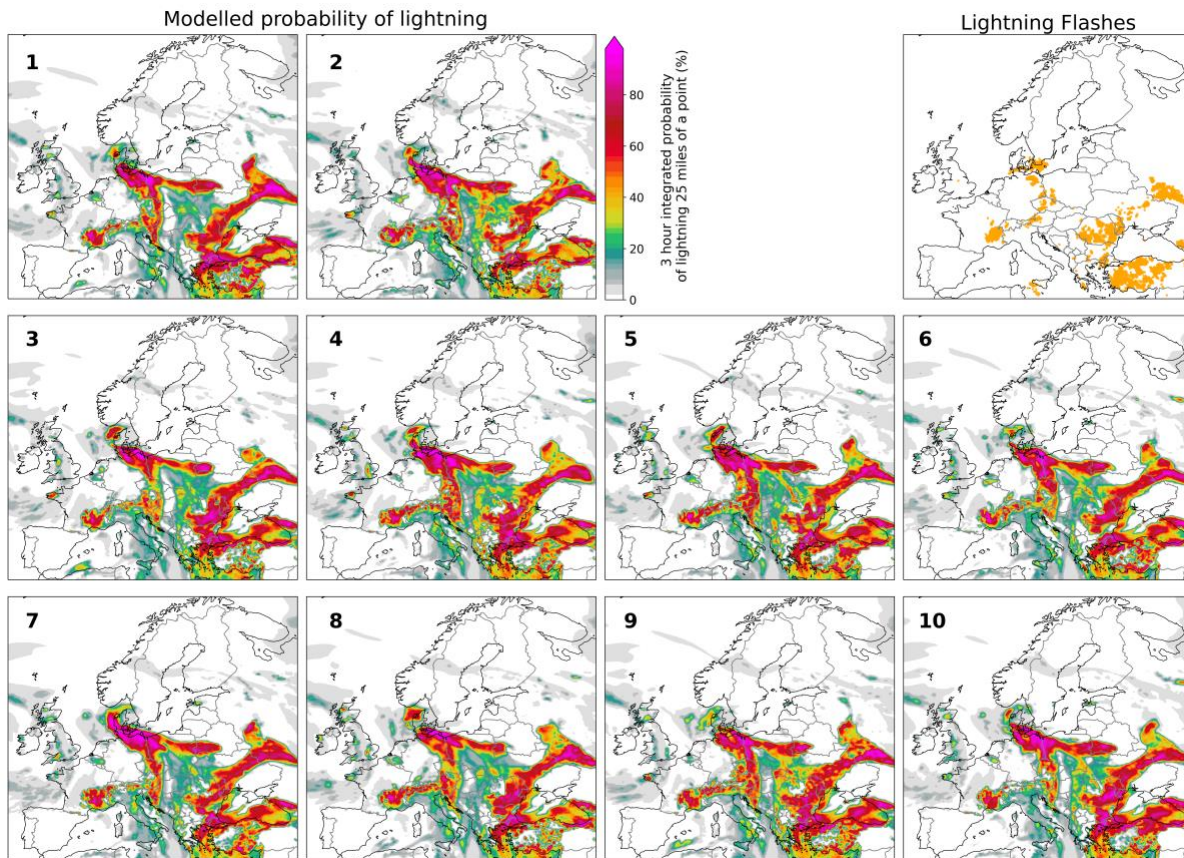
We applied AR-CHaMo for lightning and large hail to the ECMWF reforecasts to develop probabilistic ensemble forecasts for the period 2008-2019 across Europe. In a case study of the 15<sup>th</sup> of June 2019, the models provided skillful guidance both  
195 for large hail and lightning up to 108 hours. The loss of skill with increasing lead time was mostly due to increased spread in CAPE. The predictive skill was quantified in terms of AUC scores as a function of lead time: at short to medium ranges hail forecasts are highly skillful ( $\geq 0.95$  up to 60 hours) and outperform all composite indices. The skill decreases progressively, most rapidly after 108 hours in lead times. Some limitations of this study must be considered with the interpretation of these results. First, the limited vertical resolution of the ECMWF reforecasts did not allow the exact models developed using ERA5  
200 to be applied, since some of the original predictors could not be calculated due to the limited reforecast data availability. The atmospheric variables selected as predictors in place of the ERA5 ones can only approximate the original predictors and are likely not fully representative of the models developed using ERA5. It is important to note that although the original, more skilful, predictors from ERA5 could not be calculated, the adapted versions still managed to outperform state-of-the-art predictors such as SHP (at short lead times) and CAPESHEAR (at all lead times). Another limitation is that forecasts were  
205 only available four times a day, at 6 hours intervals, due to the limited temporal resolution of ECMWF re-forecasts. Given the convective nature of these events it is likely that some hail events for verification were missed in the 6-hours intervals between each forecast. To reduce this, forecasts were verified against hail reports in the three hours following the forecast time. Apart from these limitations, the developed models represent an improvement compared to state-of-the-art composite parameters in Europe. Future work will involve the application of the full ERA5 models to Numerical Weather Prediction  
210 (NWP) to develop hail forecasts operationally and on a pan-European scale. A significant improvement in predictive skill is expected with the use of the most skilful predictors calculated from the ERA5 reanalysis. An extension of this approach to different convective hazards such as severe convective wind gusts and tornadoes can also be foreseen.



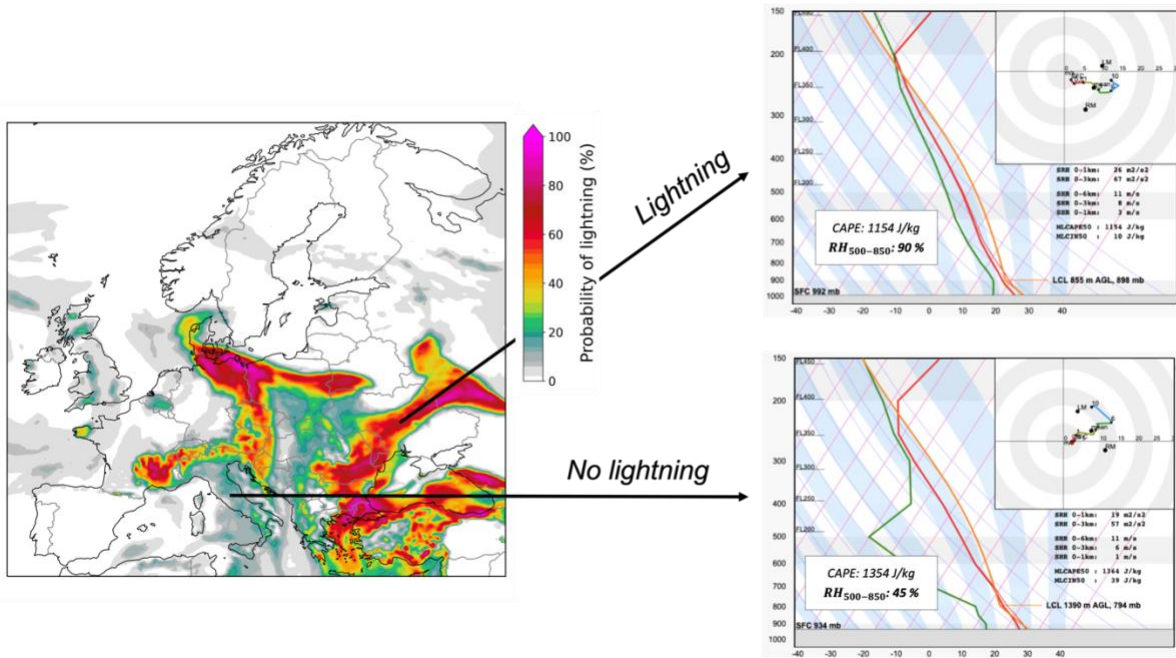


215 **Figure 1: Probabilistic forecast of hail  $\geq 2$  cm occurrence on the 15<sup>th</sup> of June 2019 at 12 UTC (initialized at 00 UTC) for the individual ensemble members. Hail reports between 12 UTC and 15 UTC are shown as triangles (green for hail  $\geq 2$  cm but  $\leq 5$  cm, black for hail  $\geq 5$  cm) in the right-top panel.**

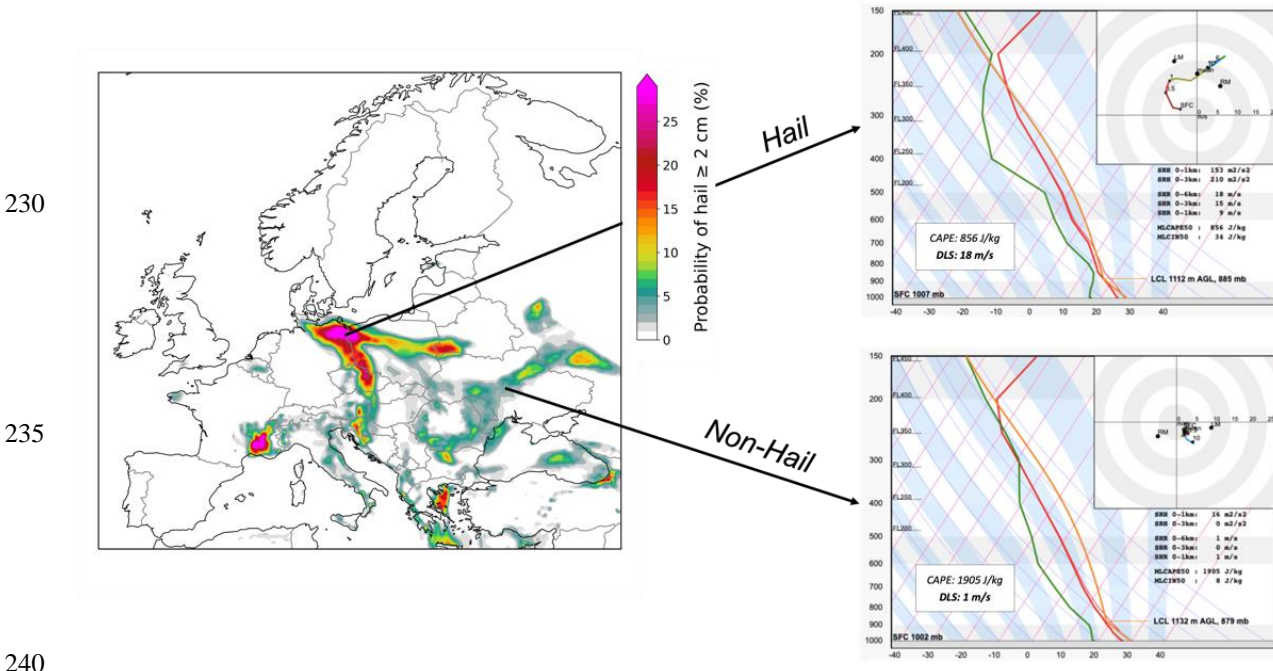




220 **Figure 2: Probabilistic forecast of lightning occurrence on the 15<sup>th</sup> of June 2019 at 12 UTC (initialized at 00 UTC) for the individual ensemble members. Lightning observations between 12 UTC and 15 UTC are shown as orange dots in the top-right panel.**



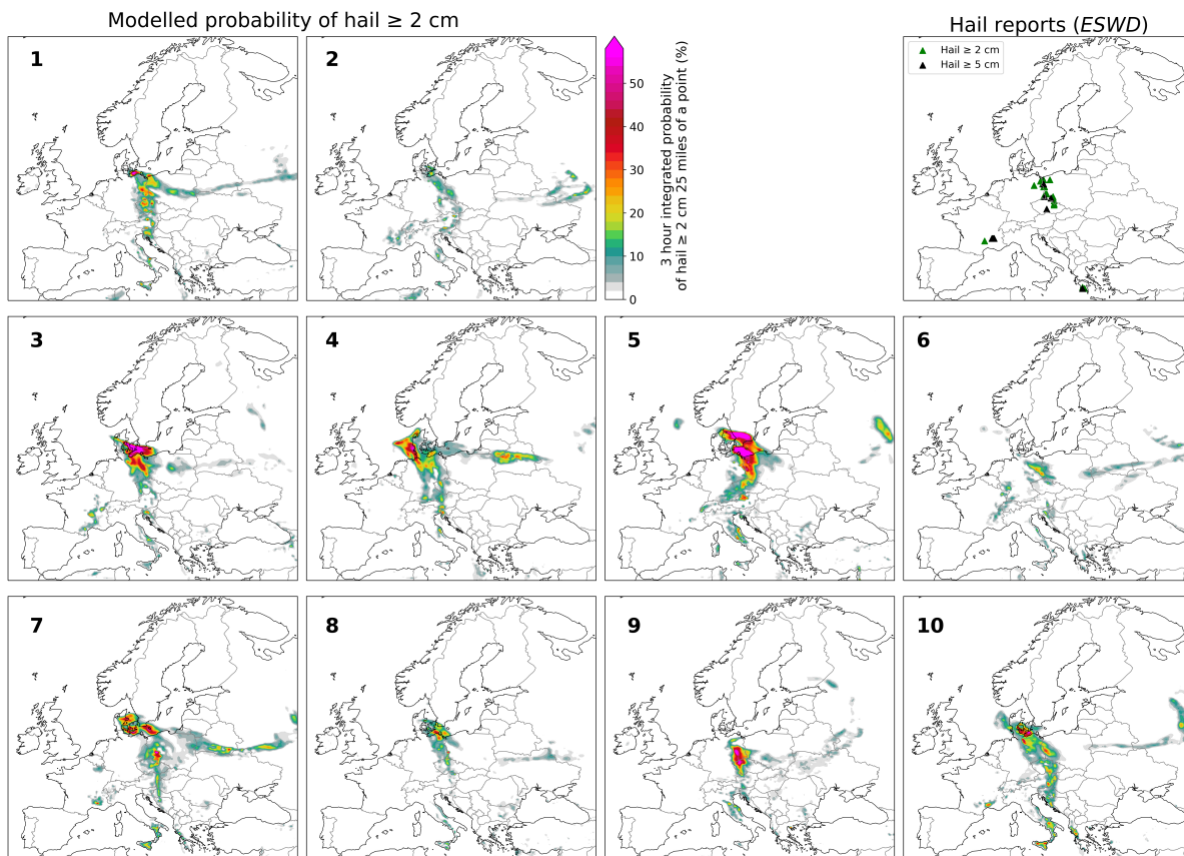
225 **Figure 3: Ensemble mean probabilistic forecast of lightning occurrence on the 15<sup>th</sup> of June 2019 at 12 UTC (initialized at 00 UTC). Forecast soundings from the ECMWF deterministic run are shown for two locations: Central Ukraine, and Central Italy. Corresponding CAPE and relative humidity between 500 and 850 hPa ( $RH_{500-850}$ ) values are also shown. Hodographs are plotted in red (0-1 km), yellow (1-3 km), green (3-6 km) and blue (6-10 km) colour for the respective height intervals.**



230  
 235  
 240 **Figure 4: Ensemble mean probabilistic forecast of hail  $\geq 2$  cm occurrence on the 15<sup>th</sup> of June 2019 at 12 UTC (initialized at 00 UTC). Forecast sounding from the ECMWF deterministic run are shown for two locations, eastern Germany, and Central Ukraine.**



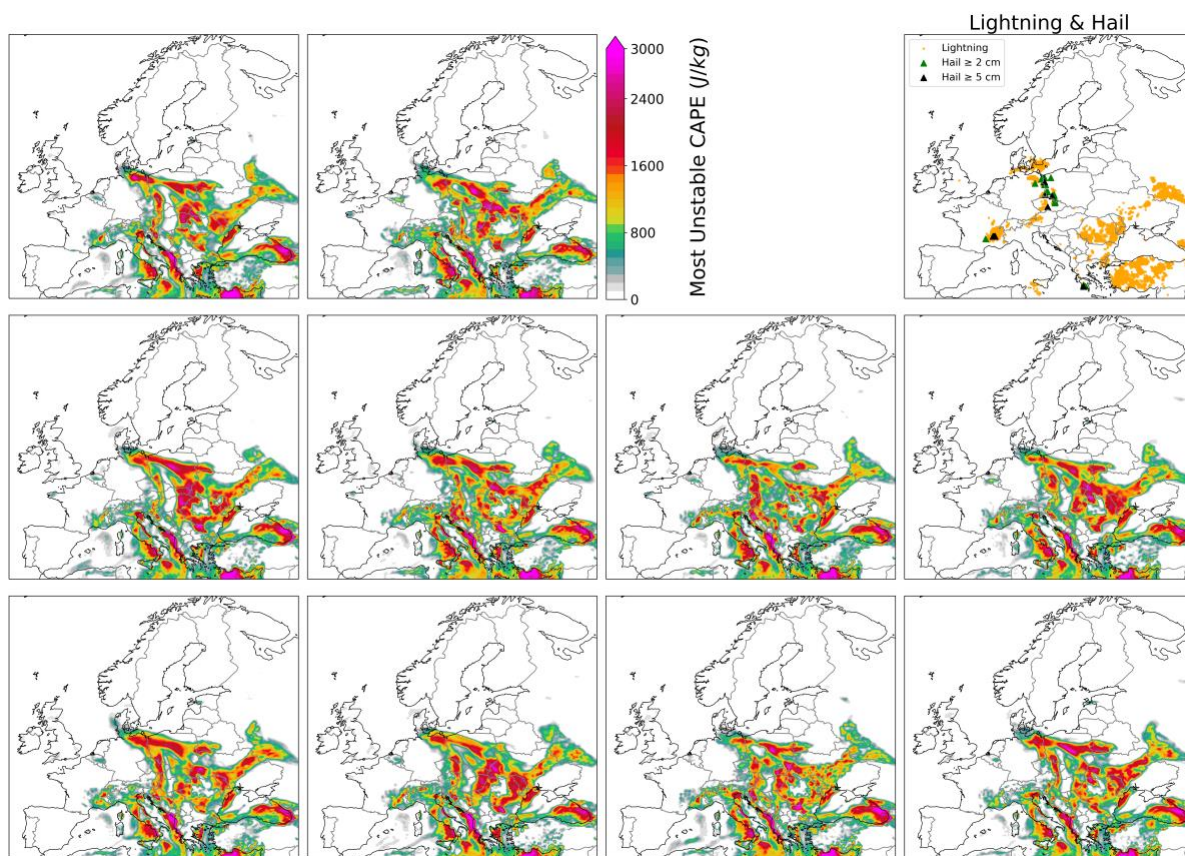
Corresponding CAPE and deep layer shear are also shown. Hodographs are plotted in red (0-1 km), yellow (1-3 km), green (3-6 km) and blue (6-10 km) colour for the respective height intervals.



245

Figure 5: As in Figure 1 but for a forecast initialized on the 11<sup>th</sup> of June 2019 at 00 UTC.





250 **Figure 6: Forecast of MUCAPE for the 15<sup>th</sup> of June 2019 at 12 UTC, initialized at 00 UTC on the same day depending on the individual ensemble members. Lightning and hail reports between 12 UTC and 15 UTC are also shown respectively as yellow dots and triangles (green for hail  $\geq 2$  cm, black for hail  $\geq 5$  cm).**

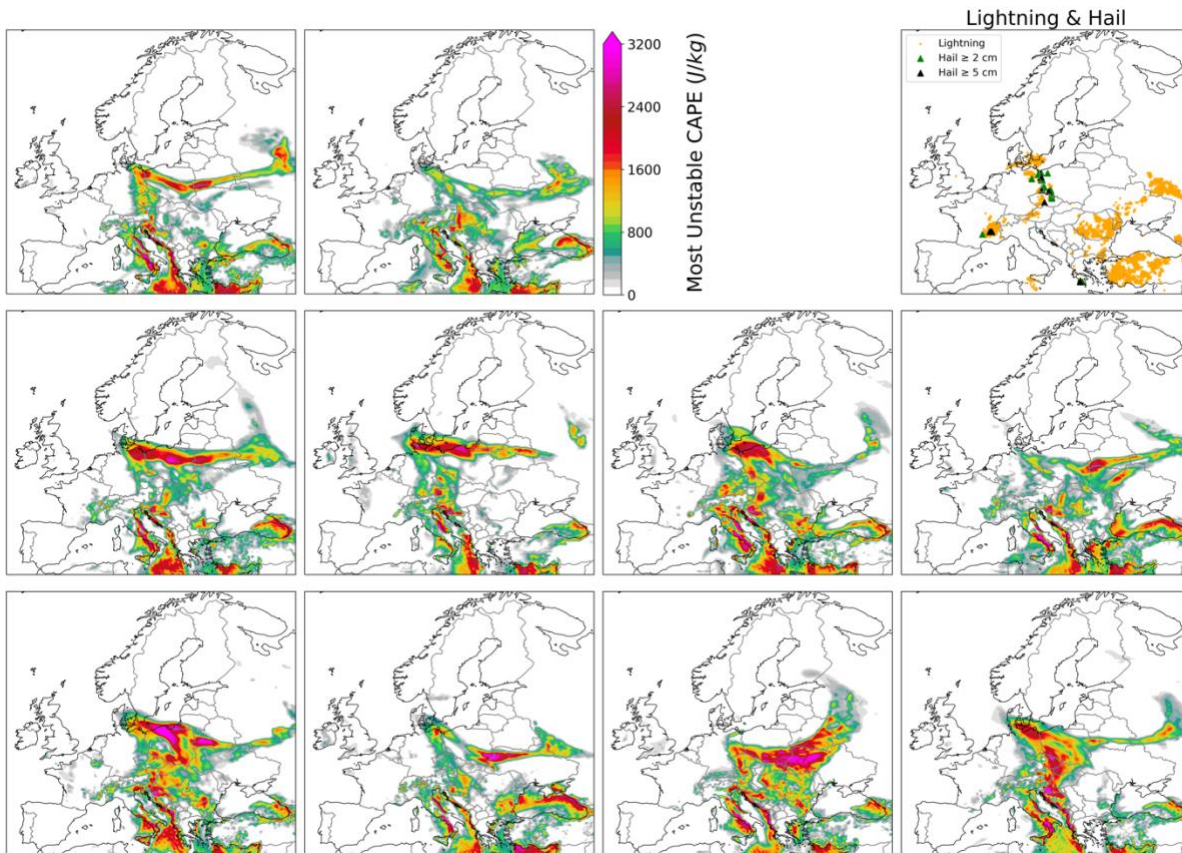
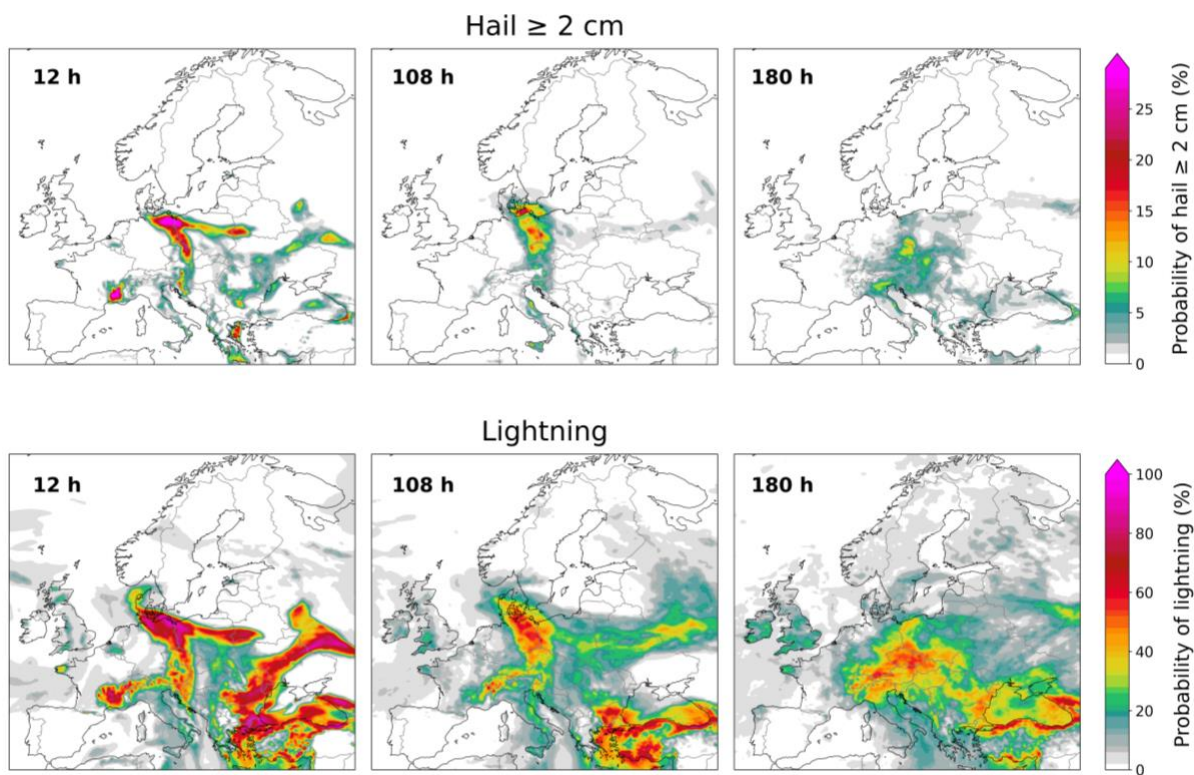
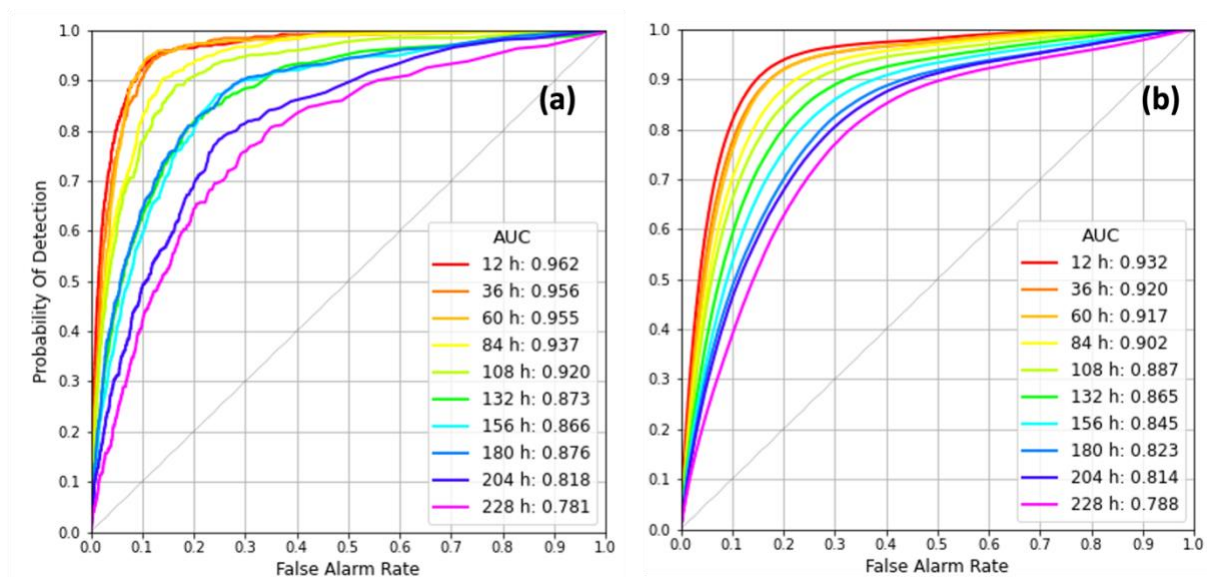


Figure 7: As in Fig. 6 for a forecast initialized on the 11<sup>th</sup> of June 2019 at 00 UTC.

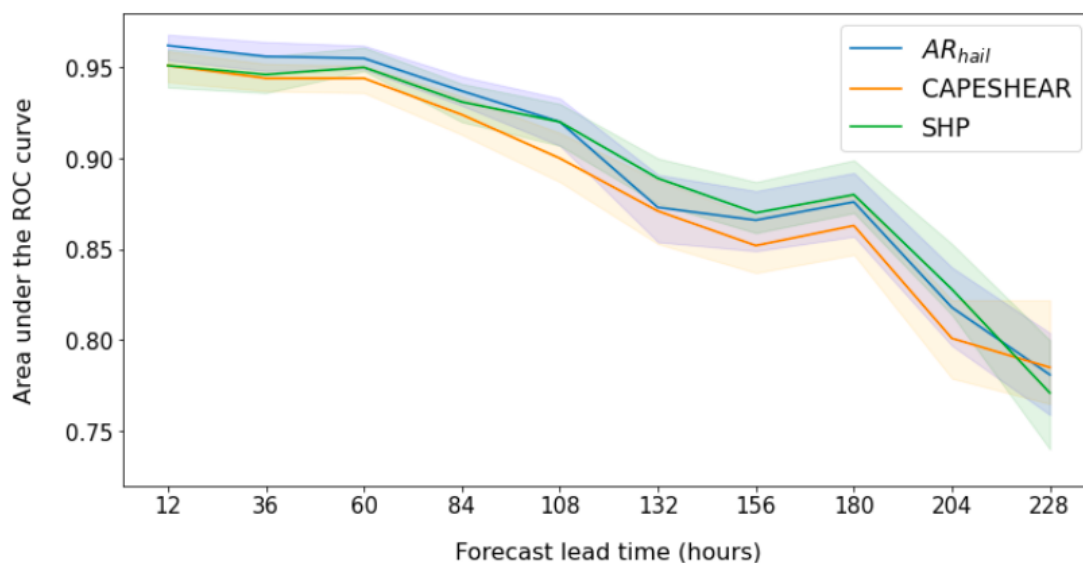


255 **Figure 8: Ensemble mean probabilistic forecast of lightning and hail  $\geq 2$  cm occurrence for three different lead times (T-12h, T-108h and T-180h).**



**Figure 9: Receiver Operating Characteristic (ROC) curve for (a) the hail  $\geq 2$  cm and (b) the lightning model for lead times from 12 to 228 hours. Corresponding values of the Area Under the ROC Curve (AUC) are also shown.**





260 **Figure 10: AUC depending on forecast lead time for  $AR_{hail}$ , CAPESHEAR and the Significant Hail Parameter. 1000-member block bootstrap was performed to estimate 95% AUC confidence intervals for each model (shaded).**

## Appendices

265 **Appendix A - ECMWF forecast sounding for the 15<sup>th</sup> of June 2019 at 12 UTC (initialized at 00 UTC) across Central Türkiye**

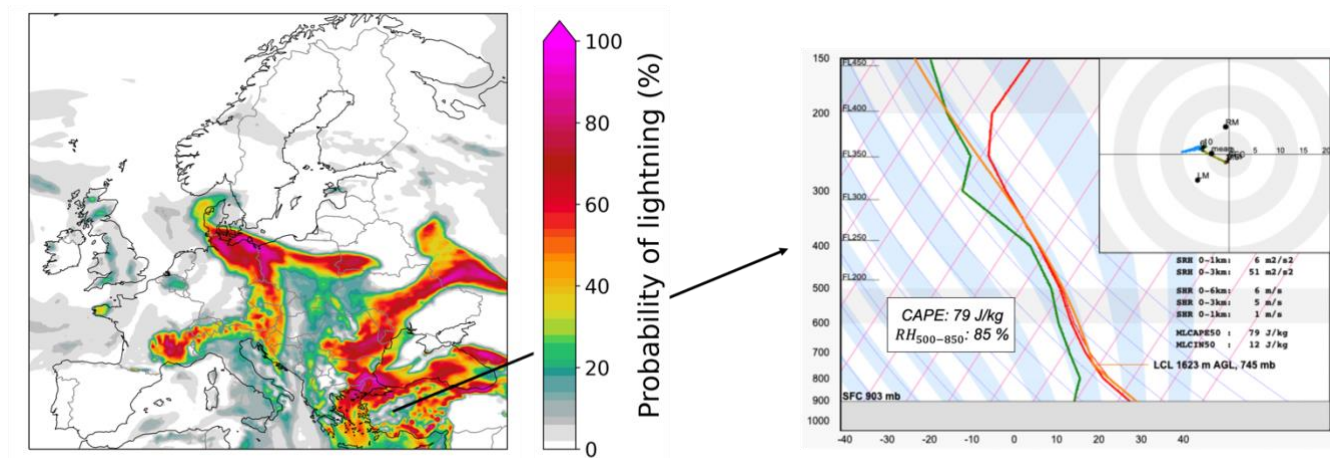
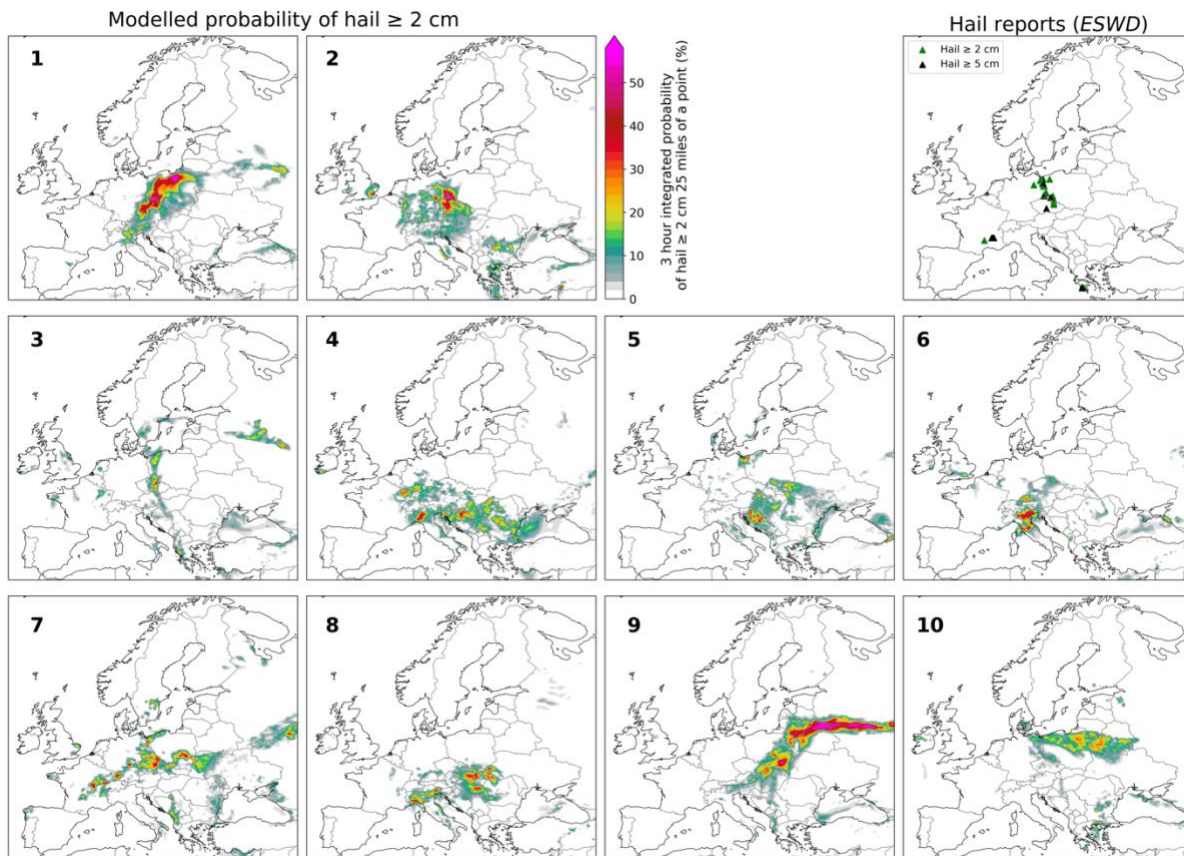


**Figure A1: Ensemble mean probabilistic forecast of lightning occurrence on the 15<sup>th</sup> of June 2019 at 12 UTC (initialized at 00 UTC). The forecast sounding from the ECMWF deterministic run is shown for Central Türkiye. The corresponding CAPE and relative humidity between 500 and 850 hPa ( $RH_{500-850}$ ) are also shown.**



### Appendix B - Additional lightning and hail forecasts for the 15<sup>th</sup> of June 2019 at 12 UTC



275 **Figure B1:** Probabilistic forecast of hail occurrence on the 15<sup>th</sup> of June 2019 at 12 UTC (on the 8<sup>th</sup> of June 2019 at 00 UTC) for the different ensemble members. Hail reports between 12 UTC and 15 UTC are also shown respectively as yellow dots and triangles (green for hail  $\geq 2$  cm but  $\leq 5$  cm, black for hail  $\geq 5$  cm) in the right-top panel.

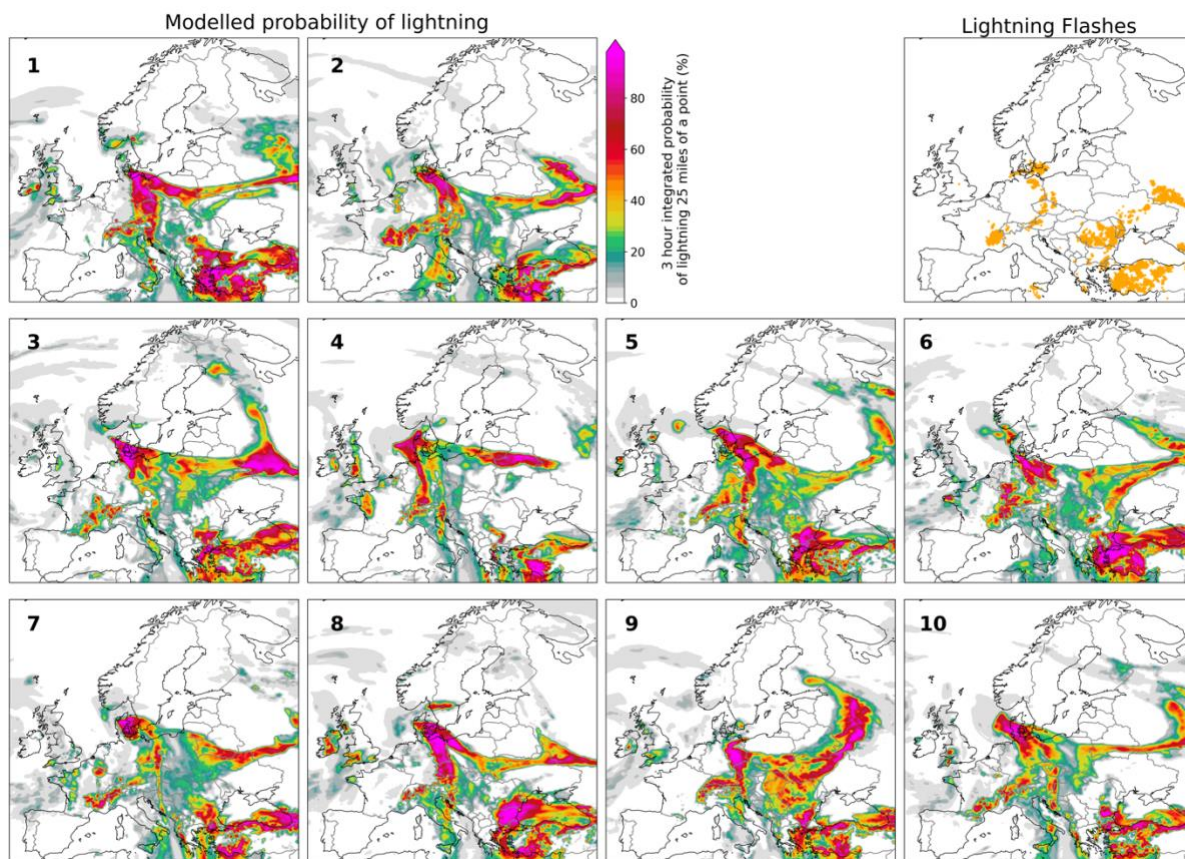
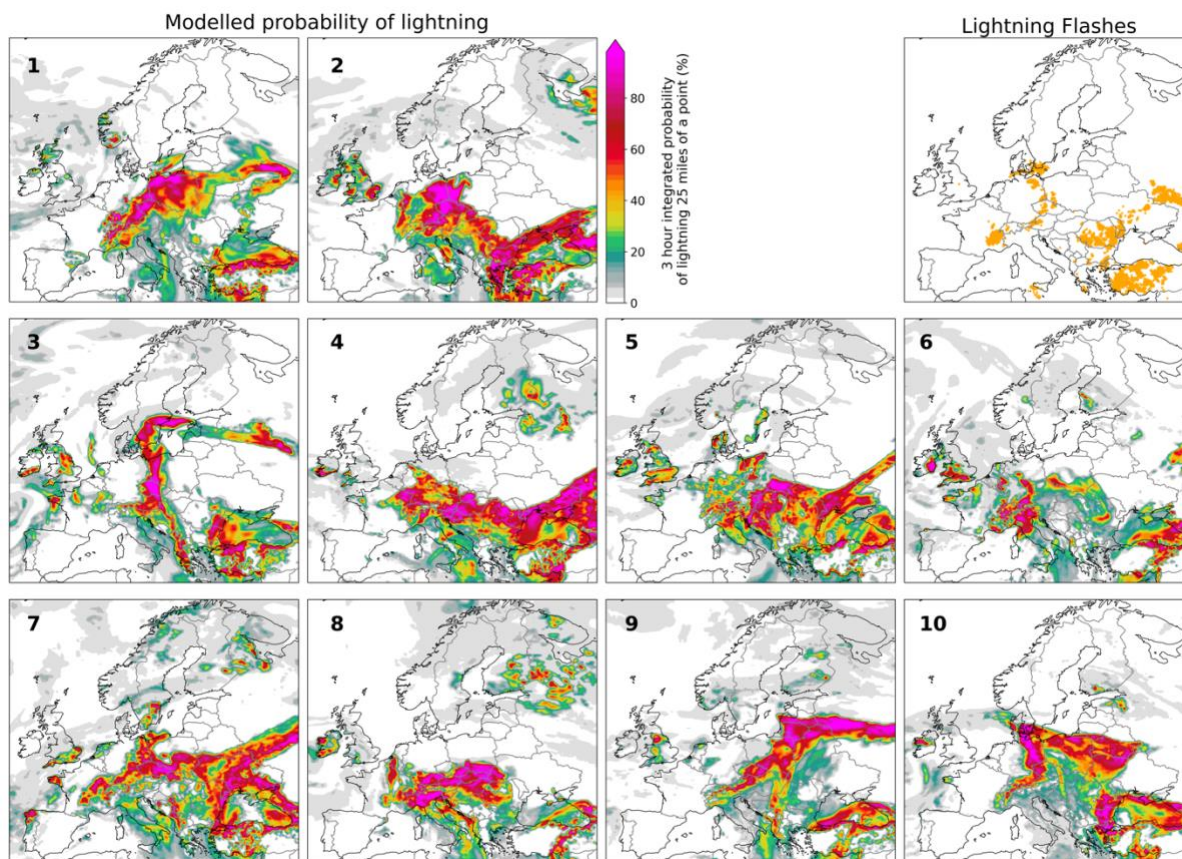


**Figure B2:** Probabilistic forecast of lightning occurrence on the 15<sup>th</sup> of June 2019 at 12 UTC (on the 11<sup>th</sup> of June 2019 at 00 UTC) for the different ensemble members. Lightning observations between 12 UTC and 15 UTC are shown respectively as yellow dots in the top-right panel.





280

Figure B3: As in B2 but for initialization on the 8<sup>th</sup> of June 2019.

### Appendix C - Acronyms of model predictors

Short name	Long name
MU_LI	Most Unstable Lifted Index
RH_500–850hPa	Mean Relative Humidity between 500 and 850 hPa
1h Acc. Conv. Precip.	1 hour Accumulated Convective Precipitation
MU_MIXR	Most Unstable Mixing Ratio
MU500_CAPE-10°	Most Unstable CAPE (for a parcel originating above 500 m AGL) released above the -10°C isotherm
EFF_MU_BS	Effective Most Unstable Bulk Shear
MU_CAPE	Most Unstable CAPE

Table C1: Acronyms for parameters from ERA5 reanalysis used in AR-CHaMo.



## 285 **Code availability**

Code for computing the probabilistic forecasts is available from the corresponding author upon request ([francesco.battaglioli@essl.org](mailto:francesco.battaglioli@essl.org)).

## **Data availability**

Probabilistic forecasts are available from the corresponding author upon request ([francesco.battaglioli@essl.org](mailto:francesco.battaglioli@essl.org)). Reforecast  
290 data are available through the ECMWF archive (<https://www.ecmwf.int/en/forecasts/dataset/operational-archive>).

## **Author contributions**

FB developed the code to compute probabilistic lightning and hail forecasts with support from PG. FB analyzed data and produced all figures. IT extracted ECMWF reforecast data. FB wrote the manuscript with revising contributions from IT, PG and TP.

## 295 **Competing interests**

The contact author has declared that neither of the authors has any competing interests.

## **Acknowledgements**

We would like to thank and acknowledge ECMWF for providing reforecast data, the Met Office for ATDnet lightning detection data and the many volunteers and ESSL staff for their reports to the ESWD. Dr. Mateusz Taszarek is acknowledged to have  
300 calculated and provided ERA5 predictors for the original AR-CHaMo models. Dr. Matthieu Chevallier is also acknowledged to have provided comments on the manuscript and have contributed to the review process.

## **Financial support**

Battaglioli's contribution to the study was funded by the German Ministry of Education and Research for project 01LP1902G "CHECC", part of the Research Programme "ClimXtreme". Groenemeijer and Púčik's contributions were funded by the  
305 Austrian Science Fund (FWF) project P33113-N "PreCAST". Tsonevsky's contribution was funded by ECMWF.

## **References**

- Adams-Selin, R. and Ziegler, C. L.: Forecasting Hail Using a One-Dimensional Hail Growth Model within WRF, Mon. Weather Rev., 144(12), 4919-4939, <https://doi.org/10.1175/MWR-D-16-0027.1>, 2016.
- Allen, J., Giammanco, I., Kumjian, M., Jurgen Punge, H., Zhang Q., Groenemeijer, P., Kunz, M., and Ortega, K.:  
310 Understanding Hail in the Earth System, Rev. Geophys., 58, <https://doi.org/10.1029/2019RG000665>, 2020.



- Anderson, G. and Klugmann, D.: A European lightning density analysis using 5 years of ATDnet data, *Nat. Hazard. Earth Sys.*, 14(4), 815-829, <https://doi.org/10.5194/nhess-14-815-2014>, 2014.
- Bang, S., and Cecil, D.: Constructing a Multifrequency Passive Microwave Hail Retrieval and Climatology in the GPM Domain, *J. Appl. Meteorol. Clim.*, 58, 1889-1904, <https://doi.org/10.1175/JAMC-D-19-0042.1>, 2019.
- 315 Battaglioli, F., Groenemeijer, P., Púčík, T., Taszarek, M., Ulbrich, U., and H. Rust, 2023: Logistic modelling of (very) large hail occurrence in Europe and the United States (1950-2021) [Manuscript submitted for publication].
- Cecil, D., and Blankenship, C.: Toward a Global Climatology of Severe Hailstorms as Estimated by Satellite Passive Microwave Imagers, *J. Climate*, 25, 687-703, <https://doi.org/10.1175/JCLI-D-11-00130.1>, 2012.
- Doswell, C. A., Brooks, H. E., and Maddox, R. A.: Flash flood forecasting: An ingredients-based methodology, *Weather Forecast.*, 11(4), 560-581, 1996.
- 320 Dotzek, N., Groenemeijer, P., Feuerstein, B., and Holzer, A. M.: Overview of ESSL's severe convective storms research using the European Severe Weather Database ESWD, *Atmos. Res.*, 93, 575–586, <https://doi.org/10.1016/j.atmosres.2008.10.020>, 2009.
- Changnon, S. A., Chagnon, D., and Hilberg, S. D.: Hailstorms across the nation: An atlas about hail and its damages. Contract Rep. 2009-12, 95 pp, 2009.
- 325 Cintineo, J., Smith, T., Lakshmanan, V., Brooks, H., and Ortega, K.: An Objective High-Resolution Hail Climatology of the Contiguous United States, *Weather Forecast.*, 27, 1235-1248, <https://doi.org/10.1175/WAF-D-11-00151.1>, 2012.
- Czernecki, B., Taszarek, M., Marosz, M., and Polrolniczak, M.: Application of machine learning to large hail prediction - The importance of radar reflectivity, lightning occurrence and convective parameters derived from ERA5, *Atmos. Res.*, 227, 249-300, <https://doi.org/10.1016/j.atmosres.2019.05.010>, 2019.
- 330 Enno, S., Sugier, J., Alber, R., and Seltzer, M.: Lightning flash density in Europe based on 10 years of ATDnet data, *Atmos. Res.*, 235, 104769, <https://doi.org/10.1016/j.atmosres.2019.104769>, 2020.
- Fluck, E., Kunz, M., Geissbuehler, P., and Ritz, S.: Radar-based assessment of hail frequency in Europe, *Nat. Hazard. Earth Sys.*, 21, 683-701, <https://doi.org/10.5194/nhess-21-683-2021>, 2021.
- 335 Gallo, B. T., Clark, A. J., and Dembek, S. R.: Forecasting tornadoes using convection-permitting ensembles, *Weather Forecast.*, 31, 273– 295, <https://doi.org/10.1175/WAF-D-15-0134.1>, 2016.
- Gallo, B. T., Clark, A. J., Smith, B. T., Thompson, R. L., Jirak, I., and Dembek, S. R.: Blended probabilistic tornado forecasts: Combining climatological frequencies with NSSL–WRF ensemble forecasts, *Weather Forecast.*, 33(2), 443– 460, <https://doi.org/10.1175/WAF-D-17-0132.1>, 2018.
- 340 Gensini, V.A. and Tippett, M.K.: Global Ensemble Forecast System (GEFS) predictions of Days 1–15 U.S. tornado and hail frequencies, *Geophys. Res. Lett.*, 46(5), 2922–2930, <https://doi.org/10.1029/2018gl081724>, 2019.
- Groenemeijer, P., and Coauthors: Severe Convective Storms in Europe: Ten Years of Research and Education at the European Severe Storms Laboratory, *B. Am. Meteorol. Soc.*, 98, 2641-2651, <https://doi.org/10.1175/BAMS-D-16-0067.1>, 2017.





- Hamill, T.M., Hagedorn, R., and Whitaker, J.S.: Probabilistic forecast calibration using ECMWF and GFS ensemble  
345 reforecasts. part II: Precipitation, *Mon. Weather Rev.*, 136, 2620–2632, <https://doi.org/10.1175/2007mwr2411.1>, 2008.
- Hersbach, H., and Coauthors: The ERA5 global reanalysis, *Q. J. Roy. Meteor. Soc.*, 146, 1999–2049,  
<https://doi.org/10.1002/QJ.3802>, 2020.
- Johnson, A., and Sugden, K.: Evaluation of Sounding-Derived Thermodynamic and Wind-Related Parameters Associated with  
Large Hail Events, *E-Journal of Severe Storms Meteorology*, 9, 1-42, <https://doi.org/10.55599/ejssm.v9i5.57>, 2014.
- 350 Jewell, R., and Brimelow, J.: Evaluation of Alberta Hail Growth Model Using Severe Hail Proximity Soundings from the  
United States, *Weather Forecast.*, 24, 1592-1609, <https://doi.org/10.1175/2009WAF2222230.1>, 2009.
- Kumjian, M., Lombardo, K., and Loeffler, S.: The Evolution of Hail Production in Simulated Supercell Storms, *J. Atmos.  
Sci.*, 78, 3417-3440, <https://doi.org/10.1175/JAS-D-21-0034.1>, 2021.
- Lepore, C., Tippet, M. K., and Allen, J. T.: ENSO-based probabilistic forecasts of March–May US tornado and hail  
355 activity, *Geophys. Res. Lett.*, 44, 9093– 9101, <https://doi.org/10.1002/2017GL074781>, 2017.
- Lepore, C., Tippet, M. K., and Allen, J. T.: CFSv2 monthly forecasts of tornado and hail activity. *Weather  
Forecast*, 33, 1283– 1297, <https://doi.org/10.1175/WAF-D-18-0054.1>, 2018.
- Loken, E. D., Clark, A. J., and Karstens, C. D.: Generating Probabilistic Next-Day Severe Weather Forecasts from Convection-  
Allowing Ensembles Using Random Forests, *Weather Forecast.*, 35, 1605-1631, <https://doi.org/10.1175/WAF-D-19-0258.1>,  
360 2020.
- Martius, O., Kunz, M., Nisi, L., and Hering, A.: Conference report 1st European Hail Workshop, *Meteorol. Z.*, 24, 441–  
442, <https://doi.org/10.1127/metz/2015/0667>, 2015.
- Murillo E., Homeyer, C., and Allen, J.: A 23-Year Severe Hail Climatology Using GridRad MESH Observations, *Mon.  
Weather Rev.*, 149, 945-958, <https://doi.org/10.1175/MWR-D-20-0178.1>, 2021.
- 365 Nisi, L., Hering, A., Germann, U., Schroer, K., Barras, H., Kunz, M., and Martius, O.: Hailstorms in the Alpine region:  
Diurnal cycle, 4D-characteristics, and the nowcasting potential of lightning properties, *Q. J. Roy. Meteor. Soc.*, 146, 4170-  
4194, <https://doi.org/10.1002/qj.3897>, 2020.
- Ortega, K. L., Krause, J. M., and Ryzhkov, A. V.: Polarimetric Radar Characteristics of Melting Hail. Part III: Validation of  
the Algorithm for Hail Size Discrimination, *J. Appl. Meteorol. Clim.*, 55(4), 829-848, [https://doi.org/10.1175/JAMC-D-15-  
370 0203.1](https://doi.org/10.1175/JAMC-D-15-<br/>0203.1), 2016.
- Poręba, S., Taszarek, M., and Ustrnul, Z.: Diurnal and Seasonal Variability of ERA5 Convective Parameters in Relation to  
Lightning Flash Rates in Poland, *Wea. Forecast*, 37(8), 1447-1470, <https://doi.org/10.1175/WAF-D-21-0099.1>, 2022.
- Pučík, T., Groenemeijer, P., Rýva, D., and Kolář, M.: Proximity Soundings of Severe and Nonsevere Thunderstorms in Central  
Europe, *Mon. Weather Rev.*, 143(12), 4805-4821, <https://doi.org/10.1175/MWR-D-15-0104.1>, 2015.
- 375 Pučík, T., Castellano, C., Groenemeijer, P., Kühne, T., Rädler, A., Antonescu, B., and Faust, E.: Large Hail Incidence and Its  
Economic and Societal Impacts across Europe, *Mon. Weather Rev.*, 147, 3901-3916, [https://doi.org/10.1175/MWR-D-19-  
0204.1](https://doi.org/10.1175/MWR-D-19-<br/>0204.1), 2019.



- Rädler, A., Groenemeijer, P., Faust, E., and Sausen, R.: Detecting Severe Weather Trends Using an Additive Regressive Convective Hazard Model (AR-CHaMo), *J. Appl. Meteorol. Clim.*, 57(3), 569-587, <https://doi.org/10.1175/JAMC-D-17-0132.1>, 2019.
- Ryzhkov, A. V., Kumjian, M. R., Ganson, S. M., and Zhang, P.: Polarimetric Radar Characteristics of Melting Hail. Part II: Practical Implications, *J. Appl. Meteorol. Clim.*, 52(12), 2871-2886, <https://doi.org/10.1175/JAMC-D-13-074.1>, 2013.
- Schmidt, M.: Improvement of hail detection and nowcasting by synergistic combination of information from polarimetric radar, model predictions, and in-situ observations. Ph.D. dissertation, Universität Bonn, 150 pp, 2020.
- 385 Taszarek, M., Allen, J., Groenemeijer, P., Edwards, R., Brooks, H., Chmielewski, V., and Enno, S.: Severe Convective Storms across Europe and the United States. Part I: Climatology of Lightning, Large Hail, Severe Wind, and Tornadoes, *J. Climate*, 33, 10239-10261, <https://doi.org/10.1175/JCLI-D-20-0345.1>, 2020(a).
- Taszarek, M., Allen, J., Púčik, T., Hoogewind, K., and Brooks, H.: Severe Convective Storms across Europe and the United States. Part II: ERA5 Environments Associated with Lightning, Large Hail, Severe Wind, and Tornadoes, *J. Climate*, 33(23),  
390 10263-10286, <https://doi.org/10.1175/JCLI-D-20-0346.1>, 2020b.
- Thompson, R. L., Edwards R., and Mead C. M.: An update to the supercell composite and significant tornado parameters, 22nd Conf. Severe Local Storms, Hyannis, MA, Amer. Meteor. Soc., P8.1.,  
[https://ams.confex.com/ams/11aram22sls/techprogram/paper\\_82100.htm](https://ams.confex.com/ams/11aram22sls/techprogram/paper_82100.htm), 2004.
- Thompson, R. L., Smith, B. T., Grams, J. S., Dean, A. R., and Broyles, C.: Convective modes for significant severe  
395 thunderstorms in the contiguous United States. Part II: Supercell and QLCS tornado environments, *Wea. Forecast.*, 27, 1136–1154, <https://doi.org/10.1175/WAF-D-11-00116.1>, 2012.
- Tsonevsky, I., Doswell, C.A., and Brooks, H.E.: Early warnings of severe convection using the ECMWF Extreme Forecast Index, *Wea. Forecast.*, 33, 857–871, <https://doi.org/10.1175/waf-d-18-0030.1>, 2018.
- Vitart, F.: Evolution of ECMWF sub-seasonal forecast skill scores, *Q. J. Roy. Meteor. Soc.*, 140, 1889–  
400 1899, <https://doi.org/10.1002/qj.2256>, 2013.
- Warren, R.A., Ramsay, H.A., Siems, S.T., Manton, M.J., Peter, J.R., Protat, A., and Pillalamarri, A.: Radar-based climatology of damaging hailstorms in Brisbane and Sydney, Australia, *Q. J. Roy. Meteor. Soc.*, 146, 505–530,  
<https://doi.org/10.1002/qj.3693>, 2020.

405